Digest of Tech. Papers The 14th Conf. (1982 International) on Solid State Devices, Tokyo

B—4—8 Buried Facet BMH AlGaAs Laser

M. Okajima, Y. Watanabe, H. Asai and N. Motegi
Research & Development Center, Toshiba Corp.
Saiwai-ku, Kawasaki 210, Japan

Buried Multi-Heterostructure (BMH) laser, which has a symmetric separate confinement heterostructure, is suitable for obtaining high output power and narrow isotropic beam divergence.[1)] Window structure lasers, which have transparent regions adjacent to the laser mirrors, are very effective for improving available optical output power.[2,3)] We investigated Buried Facet BMH (BBH) laser in order to increase available optical power of the conventional BMH laser.

Figure 1 shows the schematic drawing of the BBH laser. The mesa whose longer edge was aligned to the <1$\bar{1}$0> direction was formed by using $H_3PO_4:H_2O_2:CH_3OH=1:1:3$ solution and buried in undoped $Al_{0.35}Ga_{0.65}As$. The lateral current injection confinement was accomplished by self-alignedly formed anodic oxide film on the buried region.[1)]

Figure 2 shows a light-current characteristic of a BBH laser with 250 μm-long cavity and 15 μm-long window regions at both ends of the cavity. Output power of 135 mW was obtained under pulsed operation (1kHz, pulse width:300nsec) without catastrophic optical damage. The value is more than twice as much as the maximum output power obtained for the conventional BMH lasers with Al_2O_3 facet coatings.[1)]

Threshold current I_{th} and differential quantum efficiency η_d for the BBH laser are given as follows;

$$g_{th} = \beta\left(\frac{I_{th}}{l_\circ w}\right)^m = \alpha + \frac{1}{l_\circ}\ln\frac{1}{\sqrt{k_1k_2R_1R_2}} = \alpha + \alpha_\circ \qquad (1)$$

$$\eta_{d1,2} = \eta_i\frac{\alpha_\circ}{\alpha_\circ+\alpha}\,\frac{\sqrt{k_{2,1}R_{2,1}}}{\sqrt{k_1R_1}+\sqrt{k_2R_2}}\,\frac{1-R_{1,2}}{1-\sqrt{k_1k_2R_1R_2}} \qquad (2)$$

where R_1, R_2 are reflectivity at mirror facet, k_1, k_2 are coupling efficiency of the reflected beam from the mirror facet to the active wave guide, α is the propagation loss in the active wave guide region whose length is l_0, w is the width of the active region and η_i is internal quantum efficiency.

Three kinds of lasers were fabricated from one wafer; type A: conventional BMH laser, type B: BBH laser with window regions at both ends of the cavity, and type C: BBH laser with one window region. Table 1 shows threshold currents and differential quantum efficiencies of these three kinds of lasers. The laser A and B have almost the same η_d though the laser B has a higher I_{th} value. In the laser C, η_d for the mirror facet with window region is much larger than that for the facet without window region. These results agree with consequences from Eqs. (1) and (2). Figure 3 shows the plot of calculated coupling efficiency versus length of window region assuming Gaussian beam. θ is the angle between the buried facet and the junction plane; θ=52° is an observed value and θ=90° is for an ideal case, i.e. vertical buried facet. W_x and W_y are mode sizes in the directions parallel and perpendicular to the junction plane, respectively.

The coupling efficiency k is estimated from Eq.(2) using two η_d values of 5% and 13.6% in the laser C. Thus obtained k is 14%, which is much smaller than the calculated value of 40% for 15 μm-long window region. The discrepancy is presumably because of the Gaussian beam approximation.

Figure 4 shows the near field pattern of a BBH laser at the buried facet observed by using an objective lens of NA=0.65. The pattern indicates fundamental mode oscillation, though it has a spurious spot caused by reflection at the boundary between the $Al_{0.35}Ga_{0.65}As$ buried layer and the GaAs substrate. An inteference pattern by the reflection is observed in far field pattern, which is less significant in practical applications because of finite NA's of lens systems. The spurious spot may be eliminated by deeper mesa-etching and shorter window region.

As described above, the BBH laser is very effective to provide high output power maintaining good mode characteristics of the BMH laser.

References

1) M. Okajima et al.: Jpn. J. Appl. Phys. 21(1982) Suppl. 21-1,353

2) H. Yonezu et al.: IEEE J. Quantum Electron. QE-15(1979)775

3) H. Kumabe et al.: Jpn. J. Appl. Phys. 21(1982) Suppl. 21-1,347

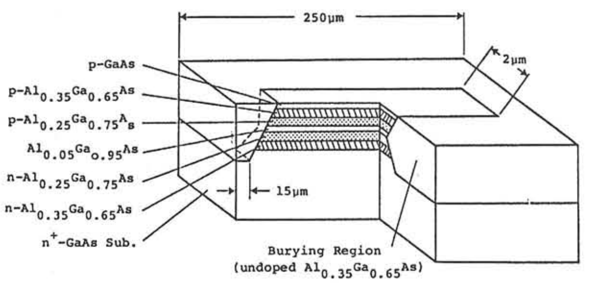

Fig.1 Schematic drawing of the BBH laser.

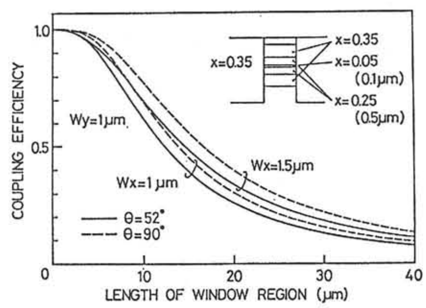

Fig.3 Calculated coupling efficiency vs length of window region.

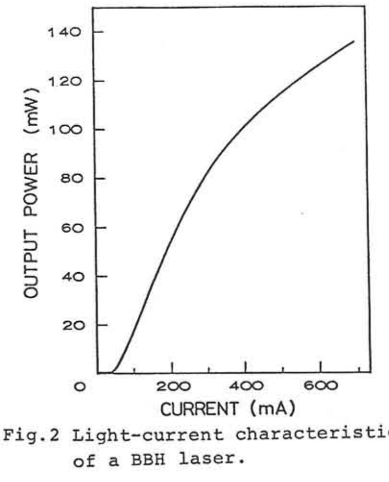

Fig.2 Light-current characteristic of a BBH laser.

Table 1
Threshold current and differential quantum efficiency for various types of BBH laser.

	I_{th}(mA)	η_d(%)
Type A	20	13.4
Type B	42	11.8
Type C	50	13.6* 5.0**

*: with window region.
**: without window region.

Fig.4 Near field pattern of a BBH laser.